# Hyperuricemia induces endothelial dysfunction and accelerates atherosclerosis by disturbing the asymmetric dimethylarginine/dimethylarginine dimethylaminotransferase 2 pathway

Tzong-Shyuan Lee [a],[*], Tse-Min Lu [b],[c], Chia-Hui Chen [a], Bei-Chia Guo [a], Chiao-Po Hsu [b],[d],[**]

[a] Graduate Institute and Department of Physiology, College of Medicine, National Taiwan University, Taipei, Taiwan
[b] Faculty of Medicine, School of Medicine, National Yang Ming Chiao Tung University, Taipei, Taiwan
[c] Division of Cardiology, Department of Internal Medicine, Taipei Veterans General Hospital, Taipei, Taiwan
[d] Division of Cardiovascular Surgery, Department of Surgery, Taipei Veterans General Hospital, Taipei, Taiwan

A R T I C L E   I N F O

A B S T R A C T

Hyperuricemia is closely associated with the mobility and mortality of patients with cardiovascular diseases. However, how hyperuricemia accelerates atherosclerosis progression is not well understood. The balance between asymmetric dimethylarginine (ADMA) and dimethylarginine dimethylaminotransferases (DDAHs) is crucial to regulate vascular homeostasis. Therefore, we investigated the role of the ADMA/DDAH pathway in hyperuricemia-induced endothelial dysfunction and atherosclerosis and the underlying molecular mechanisms in endothelial cells (ECs) and apolipoprotein E–knockout ($apoe^{-/-}$) mice. Our results demonstrated that uric acid at pathological concentrations increased the intracellular levels of ADMA and downregulated DDAH-2 expression without affecting DDAH-1 expression. Excess uric acid also reduced NO bioavailability and increased monocyte adhesion to ECs, which were abolished by using the antioxidant N-acetylcysteine, the nicotinamide adenine dinucleotide phosphate oxidase inhibitor apocynin, or DDAH-2 overexpression. In $apoe^{-/-}$ mice, treatment with oxonic acid, a uricase inhibitor, increased the circulating level of uric acid, cholesterol, and lipid peroxidation; exacerbated systemic and aortic inflammation; and worsened atherosclerosis compared with vehicle-treated $apoe^{-/-}$ mice. Furthermore, oxonic acid–treated $apoe^{-/-}$ mice exhibited elevated ADMA plasma level and downregulated aortic expression of DDAH-2 protein. Notably, DDAH-2 overexpression in the ECs of $apoe^{-/-}$ mice prevented hyperuricemia-induced deleterious effects from influencing ADMA production, lipid peroxidation, inflammation, and atherosclerosis. Collectively, our findings suggest that hyperuricemia disturbs the balance of the ADMA/DDAH-2 axis, results in EC dysfunction, and, consequently, accelerates atherosclerosis.

## 1. Introduction

Uric acid is the end product of purine metabolism; it exists majorly as urate and can be excreted through renal and gastrointestinal routes in human [1,2]. Overproduction of uric acid causes hyperuricemia, which is closely associated with the mobility and mortality of patients with cardiovascular diseases [3,4]. This causal relationship between hyperuricemia and cardiovascular disease has been established experimentally, with studies discovering that using oxonic acid to inhibit uricase in rats results in an increased plasma level of uric acid and elevated blood pressure [5,6]. Administration of hypoxanthine, the precursor metabolite of uric acid in the purine metabolic pathway, exacerbates

atherosclerosis in apolipoprotein E–knockout ($apoe^{-/-}$) mice [7]. Both basic and clinical studies have demonstrated that reducing blood uric acid levels can slow the progression of cardiovascular diseases [8,9]. These findings suggest that hyperuricemia promotes the development of cardiovascular diseases. Several mechanisms have been proposed to explain the role of hyperuricemia in vascular diseases [5,10–12]. For instance, oxidative stress mediates hyperuricemia-induced endothelial dysfunction and leads to the deregulation of vascular function and systemic inflammatory response [5,11,12]. Although these studies have highlighted the deleterious effects of hyperuricemia on vascular biology, the molecular mechanism underlying the detrimental effect of hyperuricemia is not fully understood. Thus, the molecular regulation of

---

* Corresponding author. Graduate Institute and Department of Physiology, College of Medicine, National Taiwan University, Taipei, 10051, Taiwan.
** Corresponding author. Division of Cardiovascular Surgery, Department of Surgery, Taipei Veterans General Hospital, Taipei, 11221, Taiwan.
*E-mail addresses:* ntutslee@ntu.edu.tw (T.-S. Lee), hsucp@vghtpe.gov.tw (C.-P. Hsu).

excess uric acid on endothelial dysfunction and atherosclerosis requires further investigation.

Endothelium is a continuous monolayer cell sheet lining the luminal surface of vessel walls, and it plays a key role in the maintenance of vascular functions [13,14]. Endothelium not only serves as the cross-bridge of communication between blood and cells but also actively regulates the processes and functions of surrounding cells through complex signaling pathways [15–17]. Particularly, endothelium-derived nitric oxide (NO) plays a key role in the regulation of vascular tone, modulation of inflammation, inhibition of vascular growth, platelet activation, and blood coagulation [18,19]. Disruption of endothelial function reduces the release of NO and causes increased vascular tone, enhanced inflammation, and proliferation of vascular smooth muscle cells, which all promote atherosclerosis progression [20–24]. Several studies have indicated that hyperuricemia induces endothelial dysfunction by increasing oxidative stress [25,26]; however, the underlying molecular mechanisms of hyperuricemia leading to endothelial dysfunction have yet to be clarified.

The elevated plasma level of asymmetric dimethylarginine (ADMA), an endogenous inhibitor of endothelial nitric oxide synthase (eNOS), is considered an independent biomarker and predictor of metabolic diseases [14,27,28]. In endothelial cells (ECs), ADMA can be metabolized to a less bioactive byproduct, citrulline, by using dimethylarginine dimethylaminotransferase (DDAH)-1 or DDAH-2 [29]; however, the enzymatic activity of DDAHs is impaired in the ECs of patients who have cardiovascular diseases [28]. DDAH overexpression is demonstrated to reduce ADMA levels and increase eNOS activity [30,31]. Dayoub et al. reported that DDAH-1 overexpression increases NO synthase activity, reduces systolic blood pressure and systemic vascular resistance, and increases cardiac stroke volume [32]. Lu et al. demonstrated that overexpression of DDAH-2 in ECs reduces ADMA concentration and improves eNOS activity induced by glycated protein [33]; however, the role of hyperuricemia in disrupting the balance of the ADMA/DDAH pathway to cause endothelial dysfunction and, ultimately, accelerate atherosclerosis progression is still debated.

Given the harmful effect of hyperuricemia on the vascular system, we aimed to characterize the molecular mechanism of hyperuricemia in the ADMA/DDAH pathway and delineate its involvement in hyperuricemia-induced endothelial dysfunction and atherosclerosis progression. First, we investigated the effect of high uric acid concentration on the ADMA level and DDAH expression of ECs; second, we determined whether the nicotinamide adenine dinucleotide phosphate (NADPH) oxidase (NOX)/reactive oxygen species (ROS) pathway is involved in the deregulation of the ADMA/DDAH pathway and EC dysfunction that are induced by excess uric acid; third, we explored whether DDAH-2 overexpression in ECs prevents hyperuricemia-induced EC dysfunction and atherosclerosis. Here, we provide information to clarify the pathological significance of hyperuricemia in vascular diseases.

## 2. Materials and methods

### 2.1. Reagents

Uric acid, oxonic acid, ADMA, Griess reagent, N-acetylcysteine (NAC), apocynin (APO), and mouse antibody for α-tubulin were obtained from Sigma-Aldrich (St. Louis, MO, USA). Rabbit antibodies for DDAH-1, DDAH-2, protein arginine methyltransferases 1 (PRMT1), and cationic amino acid transporter-1 (CAT-1) were obtained from Santa Cruz Biotechnology (Santa Cruz, CA, USA). Rabbit antibodies for intercellular adhesion molecule-1 (ICAM-1) and vascular cell adhesion molecule-1 (VCAM-1) were purchased from Cell Signaling Technology (Beverly, MA, USA). Our ADMA ELISA kit was obtained from Enzo Life Sciences (Farmingdale, NY, USA). Our EnzyChrom NADP$^+$/NADPH assay kit (ECNP-100) was obtained from BioAssay Systems (Hayward, CA, USA). Hydroethidine (DHE) and 2′,7′-dichlorofluorescin diacetate (DCFH-DA) were obtained from Molecular Probes (Eugene, OR, USA).

Our ELISA kits for tumor necrosis factor α (TNF-α), interleukin (IL)-1β, IL-6, monocyte chemoattractant protein 1 (MCP-1), and macrophage inflammatory protein 2 (MIP-2) were obtained from R&D Systems (Minneapolis, MN, USA).

### 2.2. Cell culture

Human aortic endothelial cells (HAECs; Cascade Biologics, Portland, OR, USA) were grown in Medium 200 (Cascade Biologics) supplemented with low-serum growth supplement (Cascade Biologics) in an atmosphere of 95% air and 5% $CO_2$ at 37 °C in plastic flasks. The final concentrations of the components in Medium 200 were 2% fetal bovine serum (FBS), 1 μg/mL hydrocortisone, 10 ng/mL human epidermal growth factor, 3 ng/mL human fibroblast growth factor, 10 μg/mL heparin, and 1% antibiotic-antimycotic mixture (penicillin, streptomycin, and amphotericin B; Gibco BRL, Carlsbad, CA, USA). The cells were used on passage numbers 3–8. THP-1 cells were obtained from the American Type Culture Collection (Manassas, VA, USA) and cultured in Roswell Park Memorial Institute (RPMI) 1640 medium supplemented with 10% FBS, 100 U/mL penicillin, and 100 μg/mL streptomycin (HyClone, Logan, UT, USA).

### 2.3. Measurement of nitrite production

The accumulated nitrite ($NO_2^-$), the stable breakdown product of NO, was measured in culture media by mixing it with an equal volume of Griess reagent and then incubating it at room temperature for 15 min. Azo dye production was analyzed by using an SP-8001 UV/VIS spectrophotometer (Metertech, Taipei, Taiwan) with absorbance at 540 nm. Sodium nitrite was used as a standard.

### 2.4. Determination of NADP$^+$/NADPH ratio

The concentrations of NADP$^+$ and NADPH and their ratios were examined using an EnzyChromTM NADP$^+$/NADPH assay kit according to the manufacturer's instructions. HAECs were treated with 12 mg/dL uric acid for 0, 5, 10, 15, 30 and 60 min. The change in NADP$^+$/NADPH ratio in the samples of cellular lysates was assessed. The fold induction is defined as the ratio of NADP$^+$/NADPH at the indicated times relative to that the time zero group set as 1.

### 2.5. Measurement of intracellular levels of ROS

The membrane-permeable probes DHE and DCFH-DA were used to assess the generation of oxidizing species. HAECs were incubated in culture medium containing DHE (10 μM) or DCFH-DA (20 μM) at 37 °C for 45 min. Uric acid stimulation was performed and repeated as necessary; thereafter, the cells were washed and detached with trypsin/EDTA, and their fluorescence intensity was analyzed by using a multi-label counter (PerkinElmer, Waltham, MA) at 518-nm excitation and 605-nm emission for ETH and at 488-nm excitation and 530-nm emission for DCF. Images were viewed using a Nikon TE2000-U fluorescence microscope (Nikon, Tokyo, Japan).

### 2.6. Adenoviral construction and infection

The replication-defective recombinant adenoviral vector that contained a human phosphoglycerate kinase (hPGK) promoter driving the human ddah-2 (Adv-ddah-2) was prepared per the protocol used in a previous study (Chen et al., 2019). ECs were infected with Adv-DDAH-2 at a multiplicity of infection (MOI) of 5–20 for 24 h and then subjected to further experiments.

### 2.7. Monocyte–EC adhesion assay

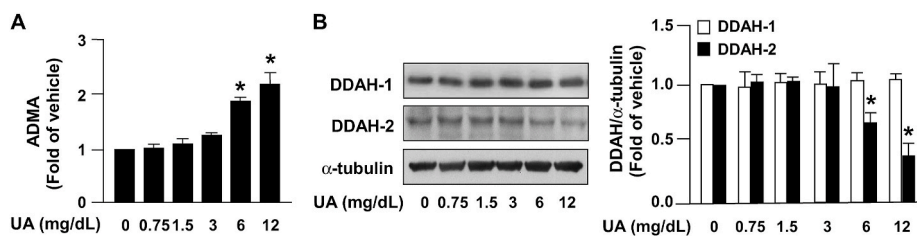Adherence of THP-1 cells to vehicle- or uric acid–treated ECs was

**Fig. 1. Excess uric acid increases intracellular levels of ADMA by reducing DDAH-2 expression in ECs.** HAECs were treated with the indicated concentrations of uric acid (UA) for 24 h. (A) Intracellular ADMA was evaluated using a commercial assay kit. (B) Western blot analysis of DDAH-1, DDAH-2, and α-tubulin. Data are expressed as means ± SEMs from five independent experiments. *Statistically significant difference ($P < 0.05$) relative to vehicle group.

performed under static conditions. For fluorescein staining, THP-1 cells were incubated with BCECF-AM at 37 °C for 1 h. After being washed, THP-1 cells were suspended in RPMI 1640 at a concentration of $1 \times 10^5$ cells/mL and incubated with ECs for 1 h, the nonadhered cells were removed, and the fluorescence intensity of cellular lysate was measured at 485-nm excitation and 530-nm emission.

### 2.8. Measurement of ADMA and inflammatory cytokines

The serum concentrations of ADMA and proinflammatory cytokines, namely TNF-α, IL-1β, IL-6, MCP-1, and MIP-2 were measured by using commercial assay kits per manufacturer instructions.

### 2.9. Western blot analysis

HAECs were lysed with SDS lysis buffer containing 1% Triton X-100, 0.1% SDS, 0.2% sodium azide, 0.5% sodium deoxycholate, and proteinase inhibitors (1 mmol/L phenylmethylsulfonyl fluoride, 10 μg/mL aprotinin, and 1 μg/mL leupeptin). Lysates were centrifuged at 12,000 rpm for 5 min, and the resulting supernatant was collected. The extracted protein was quantified through protein assay. Proteins were separated through 8% SDS-PAGE and transferred to a BioTrace polyvinylidene fluoride membrane (Pall, Cortland, NY, USA). After being blocked with 5% skim milk, blots were incubated with various primary antibodies and subsequently incubated with corresponding secondary antibodies. Protein bands were detected using an enhanced chemiluminescence kit and quantified using ImageQuant 5.2 (Healthcare Bio-Sciences, Philadelphia, PA, USA).

### 2.10. Mice

The investigation conformed to the Guide for the Care and Use of Laboratory Animals published by the US National Institutes of Health (2011), and all animal experiments were approved by the Animal Care and Utilization Committee of the National Yang-Ming University. Eight-week-old male $apoe^{-/-}$ mice were purchased from the Jackson Laboratory (Bar Harbor, ME, USA). EC-specific transgenic mouse lines were established by microinjecting Tie2-ddah-2 plasmid into fertilized C57BL/6 eggs. Positive transgenic mice were identified by performing polymerase chain reaction (PCR) tests. Tie2-ddah-2 transgenic plasmid was created by modifying Tie2-Nox4 plasmid, which was kindly provided by Dr. Junichi Sadoshima (Department of Cell Biology and Molecular Medicine, Cardiovascular Research Institute, Rutgers New Jersey Medical School, NJ, USA). To create $apoe^{-/-}$/EC-$ddah$-2 Tg mice, EC-$ddah$-2 Tg mice were crossed with the $apoe^{-/-}$ background, and PCR testing of genomic DNA was performed to confirm $apoe^{-/-}$ and EC-$ddah$-2 Tg genotypes. The mice were housed in barrier facilities maintained on a 12-h/12-h light/dark cycle. The temperature (22 °C) and humidity (40%–60%) of the vivarium were strictly controlled. The mice were group housed with three to four individuals per cage and fed a regular chow diet, which contained 4.5% fat by weight (0.02% cholesterol; Newco Distributors, Redwood, CA, USA). At 4 months old, the male $apoe^{-/-}$ and $apoe^{-/-}$/EC-$ddah$-2 Tg mice received daily treatment of

oxonic acid (100 mg/kg body weight) or saline (vehicle control) (n = 10 mice/group) through gastric gavage for 4 weeks. At the conclusion of the experiment, the mice were euthanized with $CO_2$, and their aortas were harvested and stored at −80 °C. The isolated aortas were homogenized, and the lysates obtained were subjected to Western blot analysis.

### 2.11. Quantification of atherosclerotic lesions

Mouse hearts were fixed with 4% paraformaldehyde and embedded in paraffin. To quantify atherosclerotic lesions, serial sections from the aortic roots of the mice were collected, deparaffinized, and stained with hematoxylin and eosin. Atherosclerotic lesions at the aortic sinus were photomicrographed, and their average lesion area was calculated by using Motic Images Plus 2.0 (Xiamen, China).

### 2.12. Serum lipid profile analysis

Blood was collected from live mice by performing cardiac puncture. After clotting and centrifugation were performed, the serum obtained was isolated and serum levels of cholesterol and triglycerides were measured by using the Spotchem EZ SP 4430 blood biochemical analyzer (ARKRAY, Kyoto, Japan).

### 2.13. Lipid peroxidation assay

The levels of malondialdehyde (MDA), a product of lipid peroxidation, in the aortas of $apoe^{-/-}$ mice were measured by using assay kits per the manufacturer's instructions. The results were used as a biomarker for oxidative stress.

### 2.14. Statistical analysis

The experiments were performed at least five times. Results are presented as means ± standard errors of the mean (SEM). A Mann–Whitney $U$ test was conducted to compare two independent groups. Kruskal–Wallis followed by Bonferroni post hoc analyses were conducted to account for multiple-group testing. SPSS v18.0 (SPSS, Chicago, IL, USA) was used for analyses. Differences were considered statistically significant when $P < 0.05$.

## 3. Results

### 3.1. Excess uric acid disturbs the ADMA/DDAH-2 system and results in EC dysfunction

To validate whether uric acid influences NO bioavailability in ECs, HAECs were treated using varying concentrations of uric acid (0.75, 1.5, 3, 6, and 12 mg/dL). Treatment with uric acid at pathological concentrations (6 and 12 mg/dL) increased the intracellular level of ADMA in ECs (Fig. 1A). In parallel, treatment with uric acid at pathological concentrations (6 and 12 mg/dL) reduced the protein expression of DDAH-2 without affecting DDAH-1 expression (Fig. 1B). Treatment with uric acid at concentrations of 6 and 12 mg/dL also reduced NO bioavailability and
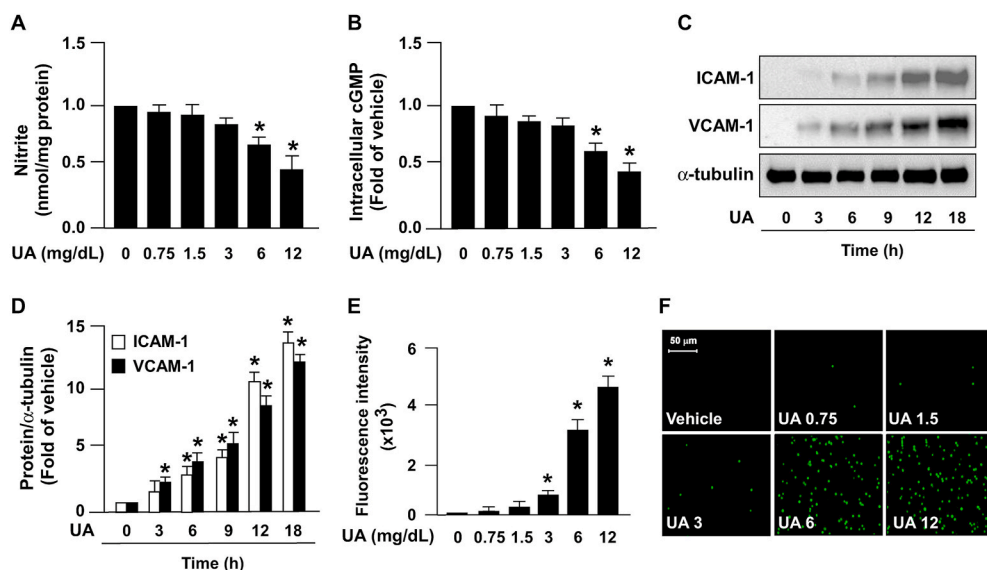
**Fig. 2. Excess uric acid induces endothelial dysfunction.** HAECs were treated with indicated concentrations of uric acid (UA) for 24 h. (A) NO bioavailability was assessed using Griess's assay, and (B) intracellular level of cGMP was evaluated using an ELISA kit. (C and D) HAECs were treated with UA (12 mg/dL) for indicated time period (0, 3, 6, 9 12, and 18 h). Protein expression of ICAM-1, VCAM-1, and α-tubulin was examined by conducting Western blot analysis. (E and F) Cells were treated with indicated concentrations of UA for 24 h and then coincubated with BCECF-AM-labeled human monocyte THP-1 cells ($1 \times 10^5$) for an additional 1 h. (E) Cellular lysates were subjected to fluorometry, and (F) cell images were photomicrographed. Data are expressed as means ± SEMs from five independent experiments. *Statistically significant difference ($P < 0.05$) relative to vehicle group.
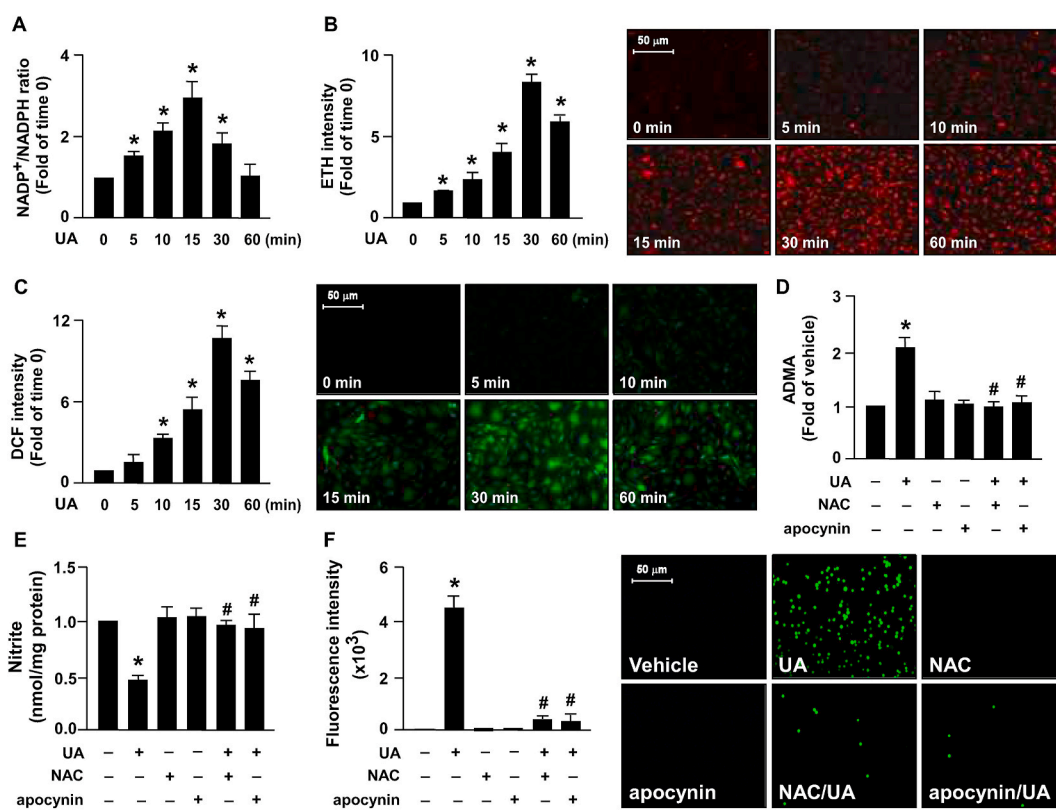


**Fig. 3. NOX/ROS pathway is crucial in the excess UA-induced deregulation of ADMA−DDAH-2 system and EC dysfunction.** HAECs were treated with 12 mg/dL uric acid (UA) for indicated time period (min). (A) The changes in $NADP^+/NADPH$ ratio was examined using the $NADP^+/NADPH$ assay kit. The fold induction is defined as the ratio of $NADP^+/NADPH$ at the indicated times relative to that the time zero group set as 1. (B and C) Intracellular levels of superoxide and hydrogen peroxide were evaluated. (D–F) HAECs were pretreated with the ROS scavenger NAC (10 mM) or the NADPH oxidase inhibitor apocynin (150 μM) for 2 h and subsequently treated with 12 mg/dL UA for 24 h. (D) Intracellular ADMA was assessed using a commercial assay kit. (E) NO production was assessed using Griess's assay. (F) Monocyte–EC adhesion assay was conducted by performing fluorometry and photomicrography. Data are expressed as means ± SEMs from five independent experiments. *Statistically significant difference ($P < 0.05$) relative to vehicle group; #Statistically significant difference ($P < 0.05$) relative to UA-treated group.

the intracellular level of cGMP (Fig. 2A and B). Moreover, uric acid dose-dependently increased the protein expression of ICAM-1 and VCAM-1 (Fig. 2C and D) and, consequently, led to increased monocyte adhesion to ECs (Fig. 2E and F); this suggests that excess uric acid impairs the physiological function of ECs. This finding suggests that a high uric acid concentration induces EC dysfunction by disrupting the balance of the ADMA/DDAH-2 system.
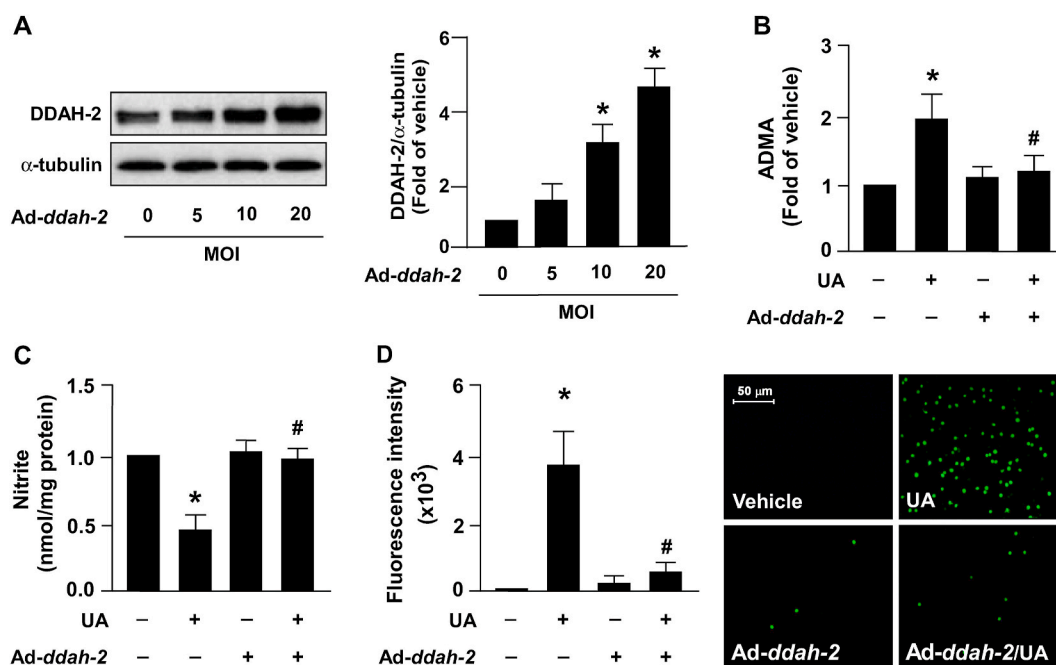
**Fig. 4.** DDAH-2 overexpression prevents excess UA-induced increases in ADMA production and EC dysfunction. (A) HAECs were infected with adenovirus expressing human *ddah-2* (Ad-*ddah-2*, 0–20 MOI) for 24 h. Western blot analysis of protein levels of DDAH-2 and α-tubulin. (B–D) HAECs were infected with Ad-vector (Ad-null) or Ad-*ddah-2* (20 MOI) for 24 h, then treated with UA (12 mg/dL) for 24 h. (B) Intracellular ADMA was assessed using a commercial assay kit. (C) NO production was assessed using Griess's assay. (D) Monocyte–EC adhesion assay was conducted by performing fluorometry and photomicrography. Data are expressed as means ± SEMs from five independent experiments. *Statistically significant difference ($P < 0.05$) relative to vehicle group; #Statistically significant difference ($P < 0.05$) relative to UA-treated group.

### 3.2. NOX/ROS signaling pathway is crucial for uric acid–induced EC dysfunction

Subsequently, we assessed the molecular mechanism by which excess uric acid deregulates the ADMA/DDAH-2 system and physiological function of ECs. An increase in NADP$^+$/NADPH ratio, which indicates the increase of NADPH oxidase activity, was observed as early as 5 min into uric acid treatment at 12 mg/dL and peaked at 15 min (Fig. 3A). In addition, 12 mg/dL of uric acid increased the production of ROS, including superoxide and hydrogen peroxide, at as early as 5 and 10 min, respectively, and led to ROS production peaking at 30 min (Fig. 3B and C). To validate that the NOX/ROS signaling pathway is essential in the uric acid–induced deregulation of the ADMA/DDAH-2 system and EC function, NOX activity and ROS production were depleted by implementing treatment with APO and NAC, respectively. Pretreatment with NAC or APO abrogated ADMA production induced by excess uric acid (Fig. 3D). Furthermore, the detrimental effect of uric acid on NO bioavailability and monocyte adhesion to ECs was abolished by NAC or NOX inhibition treatment (Fig. 3E and F). These findings suggest that NOX/ROS pathway activation is required for uric acid to have a deleterious effect on the ADMA/DDAH-2 system and EC function.

### 3.3. Overexpression of DDAH-2 alleviates excess uric acid-induced EC dysfunction in ECs

The intracellular level of ADMA in ECs is strictly regulated by DDAH-2 [29]. We thus assessed whether DDAH-2 overexpression prevents the harmful effect induced by excess uric acid on ADMA production, NO production, and monocyte adhesion to ECs. Infection with adenoviruses expressing human *ddah-2* (Ad-*ddah-2*) dose-dependently increased the intracellular protein level of DDAH-2 (Fig. 4A). In addition, DDAH-2 overexpression abolished the unfavorable effect induced by uric acid on ADMA production (Fig. 4B), NO biosynthesis (Fig. 4C) and monocyte adhesion to ECs (Fig. 4D).

### 3.4. Hyperuricemia disturbs the ADMA/DDAH-2 axis and worsens atherosclerosis in apoe$^{-/-}$ mice

To verify the *in vitro* findings and elucidate the possible effects of excess uric acid on atherosclerosis, in our *in vivo* model, the hyperlipidemia- and atherosclerosis-prone *apoe$^{-/-}$* mice were administered oxonic acid, which is the uricase inhibitor. Our results indicated that treatment with oxonic acid significantly increased the serum level of uric acid and ADMA without affecting body weight (Fig. 5A–C). Notably, treatment with oxonic acid reduced DDAH-2 protein expression without affecting DDAH1 expression in the aortas of *apoe$^{-/-}$* mice (Fig. 5D); it also worsened atherosclerosis (Fig. 5E) and hyperlipidemia, increasing the circulating levels of total cholesterol and non-high-density lipoprotein (HDL) cholesterol (Fig. 5F and G) but not affecting HDL and triglyceride levels (Fig. 5H and I). Moreover, in *apoe$^{-/-}$* mice, treatment with oxonic acid aggravated lipid peroxidation (Fig. 6A) and increased the serum levels of proinflammatory cytokines including TNF-α, IL-1β, IL-6, MCP-1, and MIP-2 (Fig. 6B) and the aortic levels of ICAM-1 and VCAM-1 (Fig. 6C). These results suggest that hyperuricemia exacerbates hyperlipidemia and inflammation and, consequently, accelerates atherosclerosis progression by disrupting the homeostasis of the ADMA/DDAH-2 axis.

### 3.5. EC-specific overexpression of DDAH-2 ameliorates atherosclerosis worsened by hyperuricemia

We created *apoe$^{-/-}$*/EC-*ddah*-2 Tg mice to determine whether DDAH-2 overexpression prevents lipid peroxidation, hyperlipidemia, inflammatory response, and atherosclerosis that are exacerbated by hyperuricemia. Compared with oxonic acid–treated *apoe$^{-/-}$* mice, DDAH-2 overexpression in ECs reduced the serum level of ADMA without changing the body weight or serum level of uric acid in *apoe$^{-/-}$*/EC-*ddah*-2 Tg mice (Fig. 7A–D). Furthermore, DDAH-2 overexpression in ECs retarded atherosclerosis progression without altering the lipid
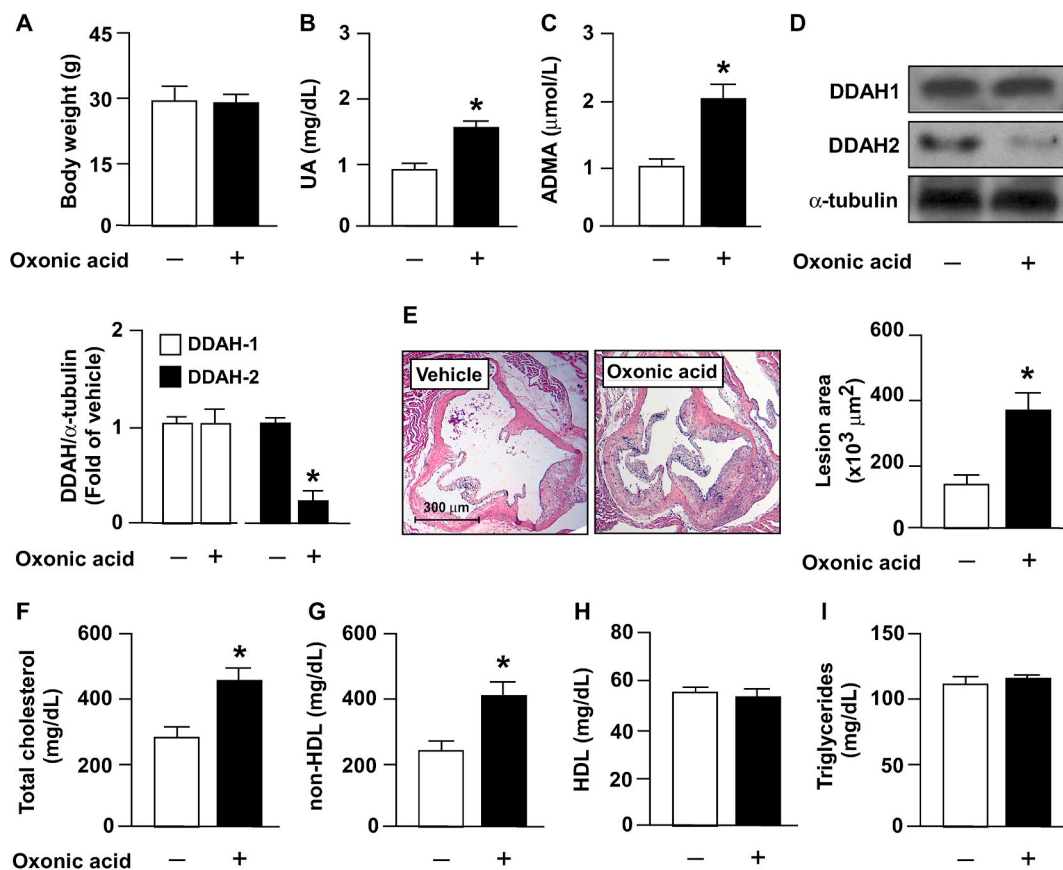
**Fig. 5.** Treatment with oxonic acid deregulates ADMA/DDAH-2 pathway and induces atherosclerosis progression in *apoe*$^{-/-}$ mice. Four-month-old *apoe*$^{-/-}$ mice received daily treatment with oxonic acid (10 mg/kg body weight) or saline (vehicle control) through gastric gavage for 4 weeks. (A) Protein levels of DDAH-1, DDAH-2, and α-tubulin in aortas. (B) Body weight. (C) Plasma levels of uric acid. (D) Plasma levels of ADMA. (E) Atherosclerotic lesion at the aortic root. (F–I) Serum levels of total cholesterol, non-HDL cholesterol, HDL cholesterol, and triglycerides. Data are expressed as means ± SEMs of 10 mice. *Statistically significant difference ($P < 0.05$) relative to vehicle-treated *apoe*$^{-/-}$ mice.
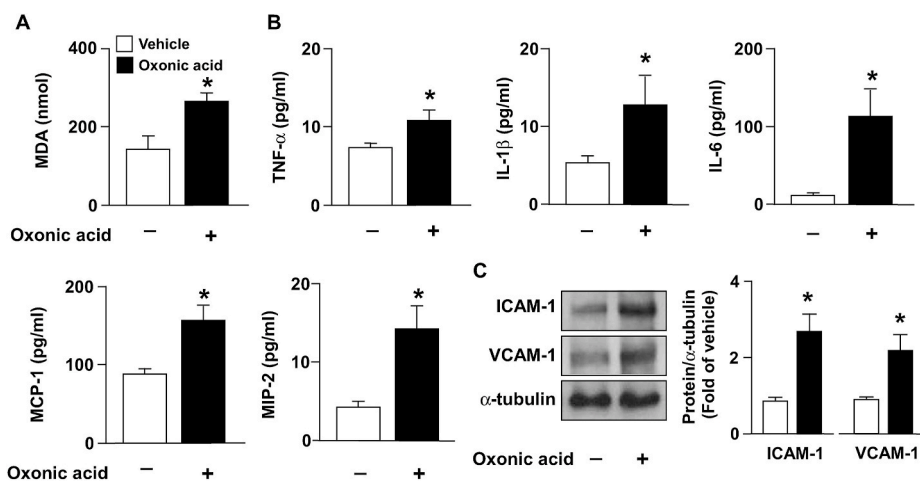


**Fig. 6.** Treatment with oxonic acid increases level of oxidative stress and inflammatory mediators in aortas of *apoe*$^{-/-}$ mice. Levels of (A) MDA, (B) TNF-α, IL-1β, IL-6, MCP-1, and MIP-2. (C) Western blots of ICAM-1, VCAM-1, and α-tubulin in aortas. Data are expressed as means ± SEMs of 10 mice. *Statistically significant difference ($P < 0.05$) relative to vehicle-treated *apoe*$^{-/-}$ mice.

profile in *apoe*$^{-/-}$/EC-*ddah*-2 Tg mice (Fig. 7E–I). Notably, DDAH-2 overexpression in ECs alleviated the lipid peroxidation and inflammatory response in *apoe*$^{-/-}$/EC-DDAH-2 Tg mice (Fig. 8A–C).

## 4. Discussion

We revealed that hyperuricemia disrupts the homeostasis of the ADMA/DDAH-2 axis and induces EC dysfunction, which lead to atherosclerosis progression. In a cell culture system, ECs were exposed to pathological concentrations (6 and 12 mg/dL) of uric acid; this caused
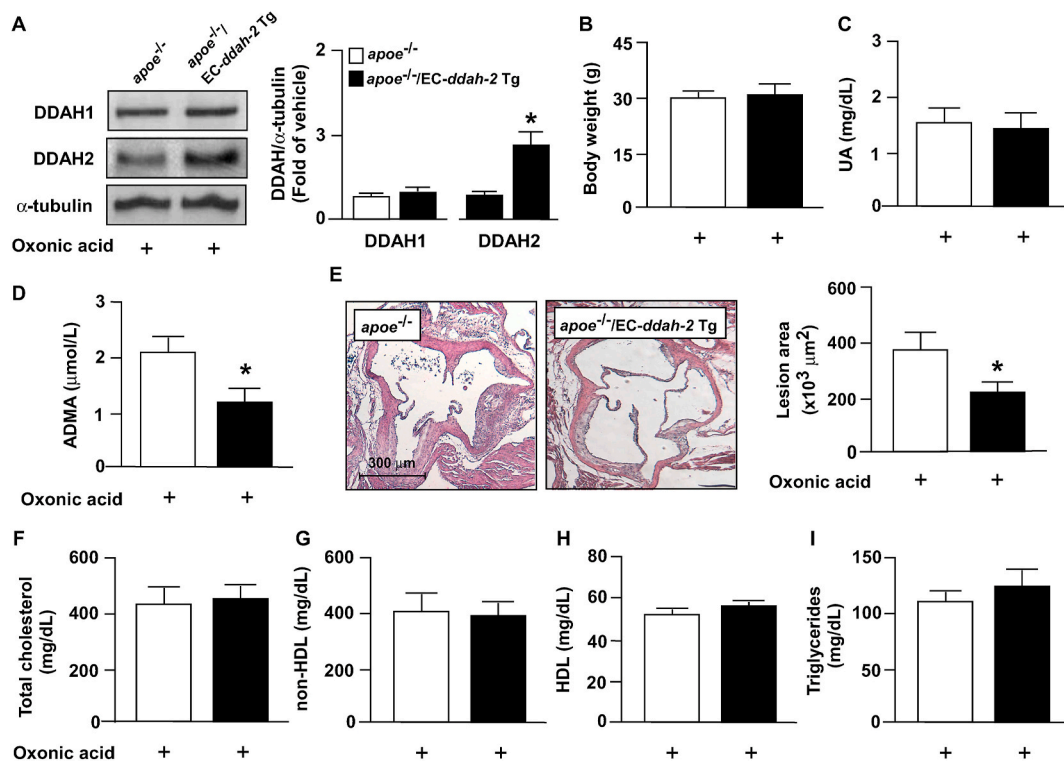
**Fig. 7.** DDAH-2 overexpression in ECs prevents detrimental effect of UA on ADMA/DDAH-2 pathway and atherosclerosis in *apoe*$^{-/-}$ mice. Four-month-old male *apoe*$^{-/-}$ mice and *apoe*$^{-/-}$/EC-*ddah*-2 Tg mice were treated daily with oxonic acid (10 mg/kg body weight) through gastric gavage for 4 weeks. (A) Body weight. (B) Plasma levels of uric acid. (C) Plasma levels of ADMA. (D) Protein levels of DDAH-1, DDAH-2, and α-tubulin in aortas. (E) Atherosclerotic lesion at the aortic root. (F–I) Serum levels of total cholesterol, non-HDL cholesterol, HDL cholesterol, and triglycerides. Data are expressed means ± SEMs of 10 mice. *Statistically significant difference ($P < 0.05$) relative to oxonic acid–treated *apoe*$^{-/-}$ mice.
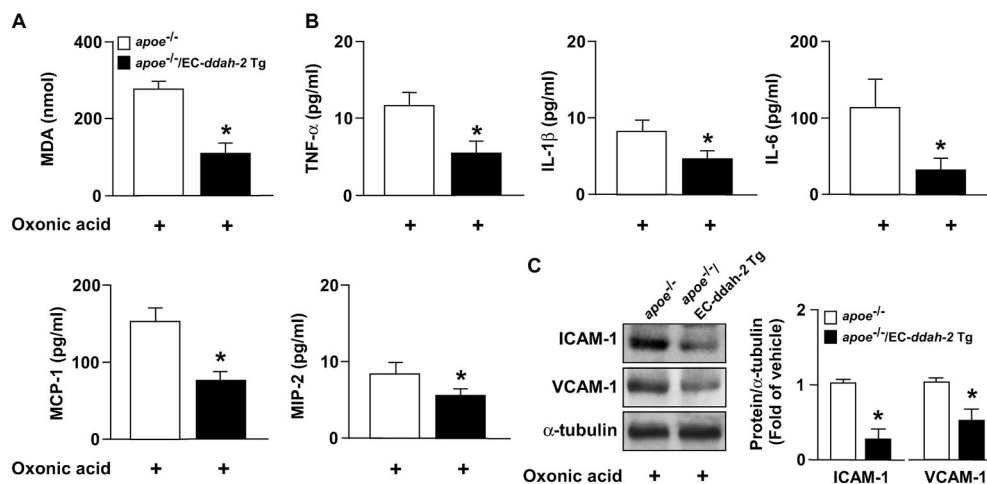


**Fig. 8.** DDAH-2 overexpression in ECs inhibits deleterious effect of UA on oxidative stress and proinflammatory response in aortas of *apoe*$^{-/-}$ mice. Levels of (A) MDA, (B) TNF-α, IL-1β, IL-6, MCP-1, and MIP-2. (C) Western blots of ICAM-1, VCAM-1, and α-tubulin in aortas. Data are expressed as means ± SEMs of 10 mice. *Statistically significant difference ($P < 0.05$) relative to oxonic acid-treated *apoe*$^{-/-}$ mice.

EC dysfunction, which was verified by the observation of impaired NO production and upregulation of adhesion molecules. Furthermore, such concentrations of uric acid significantly increased the intracellular level of ADMA through the NOX/ROS-dependent downregulation of DDAH-2 protein. The detrimental effects of uric acid on EC dysfunction were abolished by treatment with the ROS scavenger NAC, NOX inhibitor apocynin, or DDAH-2 overexpression. The *in vivo* results supported the *in vitro* observations that DDAH-2 overexpression in the ECs of *apoe*$^{-/-}$ mice prevented hyperuricemia-induced ADMA production, EC dysfunction, lipid peroxidation, inflammation, and atherosclerosis.

Thus, our findings suggest that hyperuricemia disrupts the ADMA/DDAH-2 axis in ECs and results in EC dysfunction, leading in turn to the acceleration of atherosclerosis progression. Collectively, these findings further clarify the molecular mechanisms underlying the proatherogenic effect of hyperuricemia on EC dysfunction and the pathogenesis of atherosclerosis.

Effective concentrations (6 and 12 mg/dL) of uric acid were used in our *in vitro* study to induce ADMA production, DDAH-2 downregulation, and EC dysfunction, and these concentrations were within the range of hyperuricemia. We therefore used 12 mg/dL of uric acid to examine the

effects of excess uric acid in subsequent *in vitro* experiments. Moreover, treatment with oxonic acid induced an increase in circulating uric acid by approximately 1.5-fold, which fits the clinical definition of hyperuricemia [34]. Therefore, the experimental protocols used in our *in vitro* and *in vivo* studies are relevant to clinical scenarios.

EC dysfunction characterized by a reduction of NO bioavailability and induction of adhesion molecules is the primary event in the initiation of atherosclerosis [18,19]. Prevention of EC dysfunction by activating eNOS–NO signaling is suggested to be the key mechanism that allows clinical reagents to be used in treating cardiovascular diseases [19]. For example, in addition to reducing lipid levels, statins activate eNOS and promote NO production; this suppresses the vascular inflammatory response, thereby reducing cardiovascular risks in patients [35]. By contrast, eNOS–NO signaling impairment induces EC dysfunction and results in vascular inflammation, which leads to atherosclerosis progression [18–24]. Our findings support the hypothesis that excess uric acid induces EC dysfunction by reducing NO production and increasing ICAM-1 and VCAM-1 expression and monocyte adhesion to ECs. Therefore, the deregulation of eNOS–NO signaling induced by excess uric acid, which was observed in the present study, is likely to increase vascular inflammation and worsen atherosclerosis.

Moreover, we discovered that excess uric acid and hyperuricemia reduced DDAH-2 expression and increased ADMA production in the *in vitro* and *in vivo* models, respectively. In addition to inhibiting eNOS activation and NO bioavailability, ADMA is reported to increase oxidative stress [28,36], elicit inflammation [37,38], and deregulate the cholesterol metabolism of macrophages [36]; these are key risk factors for atherosclerosis initiation and progression. Our results support the hypothesis that hyperuricemia induced by oxonic acid increased ADMA production by downregulating DDAH-2 expression in the aortas of $apoe^{-/-}$ mice. Furthermore, we revealed that, in the aortas of $apoe^{-/-}$ mice, oxonic acid upregulated the expression of PRMT1 (the key enzyme for ADMA production) but downregulated the expression of CAT-1, which has a key role in eliminating ADMA (Supplemental Fig. S1). Notably, our *in vivo* study showed that, compared with vehicle-treated $apoe^{-/-}$ mice, DDAH-2 overexpression in the ECs of oxonic acid–treated $apoe^{-/-}$ mice suppressed the hyperuricemia-induced increase in their ADMA production, thereby slowing their atherosclerosis progression. Notably, our previous study demonstrated that ADMA deregulates the cholesterol metabolism of macrophages and promotes the formation of foam cells, which are key events for the initiation and progression of atherosclerosis [36]. Sun et al. (2011) reported that ADMA is a key factor for the oxLDL-induced proliferation and migration of vascular smooth muscle cells (VSMCs) [39]. Relatedly, Hyperuricemia is reported to promote the formation of macrophage foam cells and the proliferation and migration of VSMCs [40–42]. The present study and previous studies have verified the detrimental effects of ADMA and hyperuricemia in regulating the physiological functions of vascular cells; therefore, ADMA is likely to be a key regulator in the hyperuricemia-mediated deregulation of vascular function and acceleration of atherosclerosis.

Oxidative stress plays a key mechanistic role in EC dysfunction, vascular inflammation, and the progression of vascular diseases [10–12]. Our current findings support our previous findings, that is, pretreatment with the ROS scavenger NAC or NOX inhibitor apocynin prevents ROS generation, thereby abolishing the effect of excess uric acid on ADMA production and EC dysfunction. Notably, our previous study reported that activation of NOX/ROS signaling is required for ADMA to interfere with simvastatin-conferred protection in eNOS activation [28]. Collectively, these findings suggest that the proatherogenic action of hyperuricemia results from the ADMA induced by the activation of NOX/ROS signaling in ECs. As such, antioxidant therapy targeting NOX activation or ROS clearance can be implemented to prevent the detrimental effects of hyperuricemia on EC function and atherosclerosis. Other studies have reported that antioxidants provide protective effects against cardiovascular diseases [43,44]. However, further investigations and clinical trials are required to appropriately evaluate whether antioxidant therapy prevents the detrimental effects of hyperuricemia on EC dysfunction and atherosclerosis.

Intriguingly, Hooper et al. reported that the serum level of uric acid (<5 mg/dL) in multiple sclerosis (MS) patients is lower than that of non-MS subjects [45]. Additionally, they found that increasing the level of uric acid to scavenge peroxynitrite alleviates the experimental allergic encephalomyelitis and MS in mice [45]. Moreover, Kean et al. reported that administration with uric acid effectively attenuates the peroxynitrite-mediated damage at the levels comparable to those found in the sera of normal humans (5 mg/dL) [46]. These observations suggest that adjustment of uric acid to normal levels is a potential therapeutic strategy for the treatment of neurodegenerative diseases. Nevertheless, our results indicated that the pathological concentration of uric acid (12 mg/dL) comparable to those found in the sera of hyperuricemia patients indeed increases the production of ROS and induces endothelial dysfunction. Although we cannot rule out this possibility, we thought that the activity of uric acid to scavenge peroxynitrite might not interfere with our research results.

However, our present study has several limitations. First, our *in vitro* and *in vivo* observations are not yet supported by clinical data. Second, we only investigated tissue-specific overexpression to investigate the protective role of DDAH-2 with respect to the detrimental effects of hyperuricemia on EC function and atherosclerotic progression. The specific activator or inducer of DDAH-2 is not commercially available; thus, we could not investigate the translational impact of DDAH-2 with respect to the proatherogenic effect of hyperuricemia in clinical scenarios. Nevertheless, our findings suggest that hyperuricemia deregulates EC function and accelerates the progression of cardiovascular diseases by disrupting the ADMA/DDAH-2 axis.

In conclusion, our *in vitro* and *in vivo* data suggest that the deregulation of the ADMA/DDAH-2 axis is essential in the hyperuricemia-induced activation of NOX/ROS signaling, EC dysfunction, inflammation, and the acceleration of atherosclerosis. Our findings reveal a new molecular mechanism underlying the detrimental effect of hyperuricemia on the pathogenesis of atherosclerosis; they also suggest a link between uric acid metabolism and the ADMA/DDAH-2 component of the cardiovascular system. These findings are essential for better understanding the pathological mechanism of hyperuricemia and identifying new therapeutic targets for treating atherosclerosis and related cardiovascular diseases.

## Appendix A. Supplementary data

Supplementary data to this article can be found online at https://doi.org/10.1016/j.redox.2021.102108.

## Author contributions

TS Lee, TM Lu, CH Chen, and BC Guo conducted the experiments and analyzed the data; TS Lee and CP Hsu designed the experiments and wrote the paper.

## Declaration of interests

The authors declare that they have no known competing financial interests or personal relationships that could have appeared to influence the work reported in this paper.

## Data availability

The data supporting the findings of this study are available from the corresponding author upon reasonable request.

## References

[1] J. Maiuolo, F. Oppedisano, S. Gratteri, C. Muscoli, V. Mollace, Regulation of uric acid metabolism and excretion, Int. J. Cardiol. 213 (2016) 8–14.

[2] T.T. Braga, O. Foresto-Neto, N.O.S. Camara, The role of uric acid in inflammasome-mediated kidney injury, Curr. Opin. Nephrol. Hypertens. 29 (4) (2020) 423–431.

[3] M.E. Kleber, G. Delgado, T.B. Grammer, G. Silbernagel, J. Huang, B.K. Krämer, E. Ritz, W. März, Uric acid and cardiovascular events: a mendelian randomization study, J. Am. Soc. Nephrol. 26 (11) (2015) 2831–2838.

[4] S. Zhang, Y. Wang, J. Cheng, N. Huangfu, R. Zhao, Z. Xu, F. Zhang, W. Zheng, D. Zhang, Hyperuricemia and cardiovascular disease, Curr. Pharmaceut. Des. 25 (6) (2019) 700–709.

[5] M. Mazzali, J. Kanellis, L. Han, L. Feng, Y.Y. Xia, Q. Chen, D.H. Kang, K.L. Gordon, S. Watanabe, T. Nakagawa, H.Y. Lan, R.J. Johnson, Hyperuricemia induces a primary renal arteriolopathy in rats by a blood pressure-independent mechanism, Am. J. Physiol. Ren. Physiol. 282 (6) (2002) F991−997.

[6] L.G. Sánchez-Lozada, E. Tapia, J. Santamaría, C. Avila-Casado, V. Soto, T. Nepomuceno, B. Rodríguez-Iturbe, R.J. Johnson, J. Herrera-Acosta, Mild hyperuricemia induces vasoconstriction and maintains glomerular hypertension in normal and remnant kidney rats, Kidney Int. 67 (1) (2005) 237–247.

[7] H.M. Ryu, Y.J. Kim, E.J. Oh, S.H. Oh, J.Y. Choi, J.H. Cho, C.D. Kim, S.H. Park, Y. L. Kim, Hypoxanthine induces cholesterol accumulation and incites atherosclerosis in apolipoprotein E-deficient mice and cells, J. Cell Mol. Med. 20 (11) (2016) 2160–2172.

[8] M. Volterrani, F. Iellamo, B. Sposato, F. Romeo, Uric acid lowering therapy in cardiovascular diseases, Int. J. Cardiol. 213 (2016) 20–22.

[9] F. Rahimi-Sakak, M. Maroofi, J. Rahmani, N. Bellissimo, A. Hekmatdoost, Serum uric acid and risk of cardiovascular mortality: a systematic review and dose-response meta-analysis of cohort, studies of over a million participants 19 (1) (2019) 218.

[10] J.W. Yu, T.G. Yang, W.X. Diao, X.Q. Cai, T. Li, H. Zhong, D.L. Hu, C.Q. Chen, Z. X. Chen, [Epidemiological study on hyperuricemia and gout in foshan areas, guangdong province], Zhonghua, liu xing bing xue za zhi 31 (8) (2010) 860–862.

[11] M. Jin, F. Yang, I. Yang, Y. Yin, J.J. Luo, H. Wang, X.F. Yang, Uric acid, hyperuricemia and vascular diseases, Front. Biosci. 17 (2012) 656–669, 2012.

[12] M. Kanbay, M. Segal, B. Afsar, D.H. Kang, B. Rodriguez-Iturbe, R.J. Johnson, The role of uric acid in the pathogenesis of human cardiovascular disease, Heart 99 (11) (2013) 759–766.

[13] P.F. Davies, Hemodynamic shear stress and the endothelium in cardiovascular pathophysiology, Nat. Clin. Pract. Cardiovasc. Med. 6 (1) (2009) 16–26.

[14] S. Jamwal, S. Sharma, Vascular endothelium dysfunction: a conservative target in metabolic disorders, Inflamm. Res. 67 (5) (2018) 391–405.

[15] K.A. Dora, Cell-cell communication in the vessel wall, Vasc. Med. 6 (1) (2001) 43–50.

[16] N.R. London, K.J. Whitehead, D.Y. Li, Endogenous endothelial cell signaling systems maintain vascular stability, Angiogenesis 12 (2) (2009) 149–158, 2009.

[17] A. Krüger-Genge, A. Blocki, R.P. Franke, F. Jung, Vascular endothelial cell biology: an update, Int. J. Mol. Sci. 20 (18) (2019).

[18] F. Desjardins, J.L. Balligand, Nitric oxide-dependent endothelial function and cardiovascular disease, Acta Clin. Belg. 61 (6) (2006) 326–334.

[19] L.C. Cheng, B.C. Guo, C.H. Chen, C.J. Chang, T.S. Yeh, T.S. Lee, Endothelial nitric oxide mediates the anti-atherosclerotic action of Torenia concolor Lindley var. formosama Yamazaki, Int. J. Mol. Sci. 21 (4) (2020).

[20] P. Poredos, Endothelial dysfunction in the pathogenesis of atherosclerosis, Clin. Appl. Thromb. Hemost. 7 (4) (2001) 276–280.

[21] L.C. Ching, Y.R. Kou, S.K. Shyue, K.H. Su, J. Wei, L.C. Cheng, Y.B. Yu, C.C. Pan, T. S. Lee, Molecular mechanisms of activation of endothelial nitric oxide synthase mediated by transient receptor potential vanilloid type 1, Cardiovasc. Res. 91 (3) (2011) 492–501.

[22] C. Weber, H. Noels, Atherosclerosis: current pathogenesis and therapeutic options, Nat. Med. 17 (11) (2011) 1410–1422.

[23] A. Arida, A.D. Protogerou, G.D. Kitas, P.P. Sfikakis, Systemic inflammatory response and atherosclerosis: the paradigm of chronic inflammatory rheumatic diseases, Int. J. Mol. Sci. 19 (7) (2018).

[24] J.F. Zhao, H.Y. Chen, J. Wei, S.J. Jim Leu, T.S. Lee, CCN family member 1 deregulates cholesterol metabolism and aggravates atherosclerosis 225 (3) (2019), e13209.

[25] U.M. Khosla, S. Zharikov, J.L. Finch, T. Nakagawa, C. Roncal, W. Mu, K. Krotova, E. R. Block, S. Prabhakar, R.J. Johnson, Hyperuricemia induces endothelial dysfunction, Kidney Int. 67 (5) (2005) 1739–1742.

[26] Q. Hong, K. Qi, Z. Feng, Z. Huang, S. Cui, L. Wang, B. Fu, R. Ding, J. Yang, X. Chen, D. Wu, Hyperuricemia induces endothelial dysfunction via mitochondrial Na$^+$/Ca$^{2+}$ exchanger-mediated mitochondrial calcium overload, Cell Calcium 51 (5) (2012) 402–410.

[27] D.J. Jiang, S.J. Jia, J. Yan, Z. Zhou, Q. Yuan, Y.J. Li, Involvement of DDAH/ADMA/ NOS pathway in nicotine-induced endothelial dysfunction, Biochem. Biophys. Res. Commun. 349 (2) (2006) 683–693.

[28] C.P. Hsu, J.F. Zhao, S.J. Lin, S.K. Shyue, B.C. Guo, T.M. Lu, T.S. Lee, Asymmetric dimethylarginine limits the efficacy of simvastatin activating endothelial nitric oxide synthase, J. Am. Heart Assoc. 5 (4) (2016).

[29] F. Palm, M.L. Onozato, Z. Luo, C.S. Wilcox, Dimethylarginine dimethylaminohydrolase (DDAH): expression, regulation, and function in the cardiovascular and renal systems, Am. J. Physiol. Heart Circ. Physiol. 293 (6) (2007) H3227−3245.

[30] H. Dayoub, R.N. Rodionov, C. Lynch, J.P. Cooke, E. Arning, T. Bottiglieri, S. R. Lentz, F.M. Faraci, Overexpression of dimethylarginine dimethylaminohydrolase inhibits asymmetric dimethylarginine-induced endothelial dysfunction in the cerebral circulation, Stroke 39 (1) (2008) 180–184.

[31] A.J. Pope, K. Karrupiah, P.N. Kearns, Y. Xia, A.J. Cardounel, Role of dimethylarginine dimethylaminohydrolases in the regulation of endothelial nitric oxide production, J. Biol. Chem. 284 (51) (2009) 35338–35347.

[32] H. Dayoub, V. Achan, S. Adimoolam, J. Jacobi, M.C. Stuehlinger, B.Y. Wang, P. S. Tsao, M. Kimoto, P. Vallance, A.J. Patterson, J.P. Cooke, Dimethylarginine dimethylaminohydrolase regulates nitric oxide synthesis: genetic and physiological evidence, Circulation 108 (24) (2003) 3042–3047.

[33] C.W. Lu, Z. Guo, M. Feng, Z.Z. Wu, Z.M. He, Y. Xiong, Ex vivo gene transferring of human dimethylarginine dimethylaminohydrolase-2 improved endothelial dysfunction in diabetic rat aortas and high glucose-treated endothelial cells, Atherosclerosis 209 (1) (2010) 66–73.

[34] M. Mazzali, J. Hughes, Y.G. Kim, J.A. Jefferson, D.H. Kang, K.L. Gordon, H.Y. Lan, S. Kivlighn, R.J. Johnson, Elevated uric acid increases blood pressure in the rat by a novel crystal-independent mechanism, Hypertension 3**8** (5) (2001) 1101–1106.

[35] U. Laufs, Beyond lipid-lowering: effects of statins on endothelial nitric oxide, Eur. J. Clin. Pharmacol. 58 (11) (2003) 719–731.

[36] C.H. Chen, J.F. Zhao, C.P. Hsu, Y.R. Kou, T.M. Lu, T.S. Lee, The detrimental effect of asymmetric dimethylarginine on cholesterol efflux of macrophage foam cells: role of the NOX/ROS signaling, Free Radic. Biol. Med. 143 (2019) 354–365.

[37] C. Antoniades, M. Demosthenous, D. Tousoulis, A.S. Antonopoulos, C. Vlachopoulos, M. Toutouza, K. Marinou, C. Bakogiannis, K. Mavragani, G. Lazaros, N. Koumallos, C. Triantafyllou, D. Lymperiadis, M. Koutsilieris, C. Stefanadis, Role of asymmetrical dimethylarginine in inflammation-induced endothelial dysfunction in human atherosclerosis, Hypertension 58 (1) (2011) 93–98.

[38] L. Dowsett, E. Higgins, ADMA: a key player in the relationship between vascular dysfunction and inflammation in atherosclerosis, J. Clin. Med. 9 (9) (2020).

[39] L. Sun, T. Zhang, X. Yu, W. Xin, X. Lan, D. Zhang, C. Huang, G. Du, Asymmetric dimethylarginine confers the communication between endothelial and smooth muscle cells and leads to VSMC migration through p38 and ERK1/2 signaling cascade, FEBS Lett. 585 (17) (2011) 2727–2734.

[40] D.H. Kang, S.K. Park, I.K. Lee, R.J. Johnson, Uric acid-induced C-reactive protein expression: implication on cell proliferation and nitric oxide production of human vascular cells, J. Am. Soc. Nephrol. 16 (12) (2005) 3553–3562, 2005.

[41] A. Kushiyama, H. Okubo, H. Sakoda, T. Kikuchi, M. Fujishiro, H. Sato, S. Kushiyama, M. Iwashita, F. Nishimura, T. Fukushima, Y. Nakatsu, H. Kamata, S. Kawazu, Y. Higashi, H. Kurihara, T. Asano, Xanthine oxidoreductase is involved in macrophage foam cell formation and atherosclerosis development, Arterioscler. Thromb. Vasc. Biol. 32 (2) (2012) 291–298.

[42] J.Y. Luo, D. Fu, Y.Q. Wu, Y. Gao, Inhibition of the JAK2/STAT3/SOSC1 signaling pathway improves secretion function of vascular endothelial cells in a rat model of pregnancy-induced hypertension, Cell. Physiol. Biochem. 40 (3–4) (2016) 527–537.

[43] H.N. Siti, Y. Kamisah, J. Kamsiah, The role of oxidative stress, antioxidants and vascular inflammation in cardiovascular disease (a review), Vasc. Pharmacol. 71 (2015) 40–56.

[44] K.A. Ahmad, D. Yuan Yuan, D. Nawaz, H. Ze, C.X. Zhuo, B. Talal, A. Taleb, E. Mais, D. Qilong, Antioxidant therapy for management of oxidative stress induced hypertension, Free Radic. Res. 51 (4) (2017) 428–438.

[45] D.C. Hooper, S. Spitsin, R.B. Kean, J.M. Champion, G.M. Dickson, I. Chaudhry, H. Koprowski, Uric acid, a natural scavenger of peroxynitrite, in experimental allergic encephalomyelitis and multiple sclerosis, Proc. Natl. Acad. Sci. U. S. A. 95 (2) (1998) 675–680.

[46] R.B. Kean, S.V. Spitsin, T. Mikheeva, G.S. Scott, D.C. Hooper, The peroxynitrite scavenger uric acid prevents inflammatory cell invasion into the central nervous system in experimental allergic encephalomyelitis through maintenance of blood-central nervous system barrier integrity, J. Immunol. 165 (11) (2000) 6511–6518.